

The interaction of biotic and abiotic factors at multiple spatial scales affects the variability of CO₂ fluxes in polar environments

N. Cannone^{1,2} · A. Augusti² · F. Malfasi¹ · E. Pallozzi² · C. Calfapietra^{2,4} · E. Brugnoli³

Received: 10 April 2015 / Revised: 18 December 2015 / Accepted: 19 December 2015 / Published online: 30 December 2015
© Springer-Verlag Berlin Heidelberg 2015

Abstract Climate change may turn Arctic biomes from carbon sinks into sources and vice versa, depending on the balance between gross ecosystem photosynthesis, ecosystem respiration (ER) and the resulting net ecosystem exchange (NEE). Photosynthetic capacity is species specific, and thus, it is important to quantify the contribution of different target plant species to NEE and ER. At Ny Ålesund (Svalbard archipelago, Norway), we selected different Arctic tundra plant species and measured CO₂ fluxes at plot scale and photosynthetic capacity at leaf scale. We aimed to analyze trends in CO₂ fluxes during the transition seasons (beginning vs. end of the growing season) and assess which abiotic (soil temperature, soil moisture, PAR) and biotic (plot type, phenology, LAI, photosynthetic capacity) factors influenced CO₂ emissions. NEE and ER differed between vegetation communities. All communities acted as CO₂ sources, with higher source strength at the beginning than at the end of the growing season. The key factors affecting NEE were soil

temperature, LAI and species-specific photosynthetic capacities, coupled with phenology. ER was always influenced by soil temperature. Measurements of photosynthetic capacity indicated different responses among species to light intensity, as well as suggesting possible gains in response to future increases in atmospheric CO₂ concentrations. Species-specific adaptation to low temperatures could trigger significant feedbacks in a climate change context. Our data highlight the need to quantify the role of dominant species in the C cycle (sinks or sources), as changes of vegetation composition or species phenology in response to climate change may have great impact on the regional CO₂ balance.

Keywords Arctic ecosystems · CO₂ fluxes · Species-specific photosynthetic capacity · Soil temperature · Carbon isotope composition · Climate warming

Abbreviations

A_{\max}	Light-saturated photosynthesis rate
$\delta^{13}\text{C}$	Carbon isotope composition
Δ	Carbon isotope discrimination
CTT	Climate change tower
ER	Ecosystem respiration
GEP	Gross primary photosynthesis
NEE	Net ecosystem exchange
$V_{c,\max}$	Maximum rate of Rubisco carboxylase activity

Electronic supplementary material The online version of this article (doi:10.1007/s00300-015-1883-9) contains supplementary material, which is available to authorized users.

✉ N. Cannone
nicoletta.cannone@uninsubria.it

- ¹ Department of Theoretical and Applied Sciences, Insubria University, Via Valleggio, 11, 22100 Como, CO, Italy
- ² Institute of Agro-environmental and Forest Biology (IBAF), National Council of Research (CNR), V.le G. Marconi, 2, 05010 Porano, TR, Italy
- ³ Department of Earth System Science and Environmental Technologies, National Council of Research (CNR), P.le Aldo Moro, 7, 00185 Rome, Italy
- ⁴ Czechglobe, Global Change Research Centre, Academy of Sciences of the Czech Republic, v. v. i., Bělidla 986/4a, 603 00 Brno, Czech Republic

Introduction

Since the mid-twentieth-century climate change has led to significant impacts in the Arctic, with increases in air and permafrost temperatures, snow cover decreases, and glacier

retreat (IPCC 2013). These trends are likely to continue at least until the end of the twenty-first century, as the continuing increase in greenhouse gas concentrations (especially CO₂ and CH₄) is predicted to cause further global warming (IPCC 2013). The Arctic ecosystems play a key role in the global carbon cycle (McGuire et al. 2009; Laffleur et al. 2012; Shaver et al. 2013) because northern permafrost soils account for approximately 50 % of the estimated global belowground organic carbon pool (1672 Pg, with almost 700 Pg in the first 100 cm of the soil profile) (Tarnocai et al. 2009). Therefore, in a climate change context, it is vital to track changes in the Arctic carbon balance, as the Arctic tundra may exert positive feedbacks to climate change through C release due to enhanced soil respiration (Koven et al. 2011; Euskirchen et al. 2012).

The effects of climate change on the carbon budget will depend on the balance between gross ecosystem photosynthesis (GEP), ecosystem respiration (ER) and the resulting net ecosystem exchange (NEE) (Welker et al. 2004; Chapin et al. 2006; Oberbauer et al. 2007; Laffleur et al. 2012).

The annual C budget is the result of CO₂ exchanges (gains and losses by the ecosystem) occurring during the summer, as well as during the transition and cold seasons (Lüers et al. 2014). The transition seasons (with particular emphasis on the beginning of the growing season in late spring/early summer, and on its end in late summer/early autumn) is an important focus of research, as NEE shows large fluctuations in climatic regions dominated by snow, ice and permafrost (Lüers et al. 2014). These fluctuations are strongly influenced by snow melting, soil (active layer) thawing and leaf development in spring (Uchida et al. 2010; Lüers et al. 2014), and leaf senescence and soil freezing in autumn (Christiansen et al. 2012; Lüers et al. 2014). The transition between late spring/early summer at the onset of the growing season (characterized by snow melting) is important because ecosystems shift from low, but persistent, CO₂ release under snow cover, to CO₂ uptake at and after snow melting (Lüers et al. 2014). In late summer and autumn, ecosystems may act as sinks during single-pulse events in favorable conditions, although in most cases GEP declines by 95–100 % and ER occurs at very high rates (Christiansen et al. 2012).

The contribution of winter efflux to annual soil respiration and its drivers are debated (Elberling 2007; Björkman et al. 2010; Morgner et al. 2010). Indeed, biotic and abiotic processes involved in CO₂ exchange through the snow pack are complex (Lüers et al. 2014).

The Svalbard archipelago provides a representative example of the Arctic tundra, which is characterized by highly complex and heterogeneous landscapes (McGuire et al. 2012) and high variability in soil characteristics,

moisture, vegetation and CO₂ fluxes over short spatial scales. Studies on CO₂ fluxes at different locations in this archipelago have highlighted the importance of different abiotic drivers, such as hydrological gradients (Sjögerstern et al. 2006), summer precipitation (Lloyd 2001), snow cover thickness (Björkman et al. 2010; Morgner et al. 2010), snow spatial distribution (Elberling 2007), and soil nutrients and/or organic matter (Elberling 2007; Christiansen et al. 2012). In addition, the role of water availability and/or soil moisture (Morgner et al. 2010; Uchida et al. 2010), snowmelt timing (Lloyd 2001), soil temperature (Lloyd 2001) and incident light (Uchida et al. 2010) have been studied for individual vegetation communities. Regarding the effect of biotic factors, some authors (e.g., Elberling 2007; Björkman et al. 2010; Morgner et al. 2010) have compared CO₂ fluxes between two or three different vegetation communities. Plant percentage coverage and growth (with reference to leaf development) have been considered as important drivers in controlling CO₂ fluxes (Uchida et al. 2010). Finally, Muraoka et al. (2008) analyzed the role of species photosynthetic characteristics and biomass, hypothesizing their role in contributing to ecosystem C gains and losses. The photosynthetic capacity, or the leaf photosynthetic rate either at the optimum light or temperature, is species specific and may be influenced by climate warming through changes of temperature and/or CO₂ concentration (Kirschbaum 2004; Körner 2006; Bunce 2008; Heimann and Reichstein 2008; Kositsup et al. 2009; Possell and Hewitt 2009). Species-specific photosynthetic capacity may also influence GEP (Muraoka et al. 2008; Arndal et al. 2009) and, consequently, NEE. In particular, the maximum rate of Rubisco carboxylase activity ($V_{c,max}$) and the maximum rate of photosynthetic electron transport (J_{max}) allow accurate description of plant photosynthetic capacity at the leaf level under non-limiting light conditions (Fan et al. 2011). Moreover, taking into account the inter-specific differences in $V_{c,max}$ and J_{max} will permit an increase in the accuracy of global carbon budget estimation models for terrestrial ecosystems (Fan et al. 2011). As NEE is the balance between GEP and ER, the vegetation community is a key factor because it also influences the characteristics, amount and decomposition potential of soil organic carbon (SOC), with further large implications on ER (Elberling 2007).

Moreover, photosynthetic performances may be associated with the carbon isotope composition ($\delta^{13}C$) of plant material. This is because $\delta^{13}C$ in plants is a function of the $\delta^{13}C$ of the CO₂ entering the plant and of the fractionation processes occurring during CO₂ diffusion in the leaf, photosynthetic metabolism and post-photosynthetic processes (Farquhar et al. 1989; Brugnoli and Farquhar 2000; Cernusak et al. 2013). Carbon isotope composition of plant organic matter is related to the different photosynthetic pathways (Bender 1971) and can be used to differentiate C₃ from C₄

species. Furthermore, carbon isotope discrimination (Δ) describes the variations in isotope composition caused only by the plant, eliminating the variation caused by the isotope composition of the atmospheric CO₂. The Δ value of leaf material in C₃ species has been shown to be positively related to the ratio between intercellular and atmospheric CO₂ concentration (C_i/C_a), a key parameter describing the photosynthetic performance of a leaf integrated over the period of tissue formation (O’Leary 1981; Farquhar et al. 1982; Bruognoli et al. 1998, Schmidt et al. 2015). The Δ value of plant material from Arctic species can be used as tool, associated with photosynthetic analysis, to monitor the photosynthetic performances of such species.

Studies on the transition seasons are not currently available for tundra ecosystems in the Svalbard archipelago, and thus, it is not possible to assess the contribution of different vegetation communities in terms of both abiotic (soil temperature, soil moisture, PAR) and biotic (vegetation community, target species photosynthetic capacity, leaf area index—LAI—phenology) influences on NEE, ER and GEP.

Here, we provide new data on CO₂ fluxes during the transition seasons on Svalbard, comparing the late spring/early summer (beginning of the growing season, BGS) with the late summer/autumn (end of the growing season, EGS). We hypothesized that trends in these fluxes would be different in the two seasons (in particular that NEE would be positive or less negative at BGS than at EGS and that ER would be higher at BGS than at EGS), as well as the factors most significantly affecting NEE and ER.

Further, we analyzed and compared photosynthetic performances in target species of selected vegetation communities to identify which biotic factors (plot type, photosynthetic capacity of the target species at the leaf scale, phenology, LAI) were most important in influencing NEE, as we also hypothesized that species-specific characteristics may play an important role in shaping the overall vegetation CO₂ fluxes.

To address these aims, we carried out a series of field studies near Ny Ålesund (Brogger Peninsula, Svalbard archipelago), where we selected different vegetation communities representative of the High Arctic tundra. In late summer 2012 (EGS) and late spring/early summer 2013 (BGS), we measured CO₂ fluxes at the plot scale under the selected communities and, during the summer 2013 campaign, we also measured photosynthetic performance at the leaf scale of targeted plant species.

Materials and methods

Study area

The study area was located in the Brøgger Peninsula (78°57’N; 11°34’E) close to Ny Ålesund, West

Spitsbergen, Svalbard archipelago, Norway. The mean annual air temperature at Ny Ålesund is −4.2 °C, with mean monthly air temperatures around −13 °C in January and 5 °C in July, and annual precipitation of about 433 mm (water equivalent). Spring snowmelt generally occurs in early June, and snow starts to accumulate again in late August (Boike et al. 2008; Yoshitake et al. 2010). The geological substrate includes quaternary carbonate deposits, mainly comprising marine beach deposits and weathered material or colluviums and, to a lesser extent, alluvial debris and peat. In this area, continuous permafrost underlies coastal areas to depths of about 100 m and mountainous areas to depths >500 m (Boike et al. 2008), with an active layer 0.3–1.8 m thick (André 1993).

The study site lies in polar semi-desert (Bliss and Svoboda 1984), located in the mid-Arctic vegetation region. Within this region, two different vegetation zones are recognized, identified by the presence of the characteristic species *Cassiope tetragona* (L.) D. Don and *Dryas octopetala* L. (Ronning 1986). Both zones are characterized by the occurrence of different vegetation series. In the study site, three main vegetation series (Ronning 1986) occur: (1) ridge vegetation; (2) snow-bed vegetation; and (3) heath vegetation. The distribution of the different vegetation series follows environmental gradients mainly related to the thickness and persistence of snow cover and the ground moisture regime during summer (Elvebakk 1994, Sjögerstern et al. 2006), as well as to the occurrence and characteristics of periglacial features (Cannone et al. 2004). Each vegetation series includes several communities. The ridge vegetation is typified by mesic conditions and consists of two communities dominated by *D. octopetala* and *C. tetragona*, respectively. The snow-bed vegetation is associated with moderate snow cover persistence and consists of a community dominated by *Salix polaris* Wahlenb. The heath vegetation mainly occurs where less snow accumulates and snow melt occurs earlier and includes two primary vegetation communities characterized by *Carex rupestris* All. or *Saxifraga oppositifolia* L.

Field measurements: CO₂ fluxes

Field measurements were carried out in 2012 and 2013 close to Ny Ålesund. In 2012, we performed preliminary analyses focusing on the end of the growing season (late summer, August 1–15, 2012, EGS) to assess whether the CO₂ fluxes exhibited a spatial variability among different vegetation communities and active layer thickness conditions. For this purpose, we selected communities representative of different ecological conditions relating to active layer thickness, snow cover and ground thermal regime as documented in the available literature (Ronning 1986; Elvebakk 1994; Cannone et al. 2004; Sjögerstern

et al. 2006). During 2012, the field measurements were carried out at the plot scale at two different sites separated by about 2 km and termed climate change tower site (CCT) and Strandvatnet (SND). In this part of the study, we analyzed vegetation communities, with one plot at CCT and one plot at SND, dominated by the following species: (a) *C. tetragona*; (b) *D. octopetala*; (c) *S. polaris*; (d) *S. oppositifolia*; (e) *C. rupestris*. Based on the preliminary results of the 2012 campaign, which indicated that these different vegetation communities were characterized by different NEE and ER, measurements were carried out in the spring 2013 field campaign (7 June–13 July, BGS) at the CCT site. These measurements started from the snow melting and ended before the vegetation peak was reached (i.e., when leaf development is completed and photosynthetic activity reaches its maximum, typically mid- to late July). The decision to restrict observations to a single site was made in order to minimize impacts on these fragile terrestrial ecosystems, based on the observation that the 2012 data showed limited spatial variability between the two sites (CCT vs. SND). The five plots that were therefore analyzed in both 2012 and 2013 were located on a flat area about one hundred meters distant from CCT and separated by 20–50 m from each other. They were situated on the same type of deposits and possessed similar morphologic and topographic conditions.

Measurements of CO₂ fluxes at the leaf scale were also carried out in 2013 in order to assess the photosynthetic capacity of individual target species.

CO₂ fluxes at the plot scale

CO₂ exchange measurements were performed using a portable automated CO₂ exchange station (ACE, ADC BioScientific Ltd., <http://www.adc.co.uk>) linked with an infrared gas analyzer (IRGA). It was operated in open mode with zero option. The open mode measures the rate of change of CO₂ concentration of the gas in the chamber during the assay. The zero option measures the ambient CO₂ and is used to recalculate ambient CO₂ and position the stored values on the linearization curve, providing a more precise value of NEE (net ecosystem exchange) and ER (ecosystem respiration). Stainless-steel soil collars (230 mm diameter) were inserted in the soil prior to the start of the measurements in each of the selected plots, reaching a standard depth of 4 cm. Both in 2012 and 2013, the soil collars were inserted 2 days before the start of the measurements. They remained in the soil throughout the season and were removed only at the end of the entire campaign.

The CO₂ exchange was measured: (a) under ambient light conditions to determine NEE and (b) with a covered chamber (complete darkness) to measure ER (ecosystem

respiration). Between measurements, the chamber was opened and the canopy was ventilated. A typical sequence/cycle included two consecutive measurements under ambient light (NEE), followed by one dark measurement (ER). Gas exchange rates are expressed on a ground area basis as $\mu\text{mol CO}_2 \text{ m}^{-2} \text{ s}^{-1}$. ER values are always positive, showing a release of CO₂ from the ecosystem to the atmosphere. The NEE may show either positive or negative values: when $\text{NEE} < 0$, the ecosystem incorporates CO₂ from the atmosphere (when gross ecosystem photosynthesis, GEP, exceeds ER), and when $\text{NEE} > 0$, there is a release of CO₂ from the ecosystem to the atmosphere (when ER exceeds GEP). Using the measured values for NEE and ER, we calculated GEP using the equation $\text{GEP} = \text{NEE} - \text{ER}$. At the same time that CO₂ exchange rate analyses took place, soil temperature (thermistors, ADC Bioscientifics) and soil moisture at 2 cm depth (moisture sensors Decagon Echo) were recorded. Photosynthetically active radiation (PAR) was measured using a silicon photocell located on the top of the operating arm of the chamber (30 cm above the ground surface). Soil temperature, soil moisture and PAR were measured continuously during each assay of the CO₂ fluxes (which lasted at least 15 min) both for NEE and for ER. On each day, NEE and ER were measured at a minimum of four different times between 09.00 and 16.00 (Ny Ålesund local time). For the full characterization of each plot selected, we sampled both the phytomass and the underlying soil for laboratory analyses at the end of the field campaign. In 2013, species phenology [seasonal life cycles, such as first shoot, new leaves (greening stages), first flower, flower anthesis and main flowering (reproductive stages), seed development] was analyzed following the protocol of the international tundra experiment (ITEX) (Molau and Molgaard 1996). For each target species in each plot, the Leaf Area Index (LAI, here defined as the amount of leaf area in a canopy per unit ground area) was measured as the one-sided LAI (Barclay 1998) through an optically based area measurement system (Asner et al. 2003).

Plant photosynthetic capacity at the leaf scale

CO₂ exchange rates were measured at the leaf scale on four selected species (*D. octopetala*; *S. polaris*; *C. rupestris*; *S. oppositifolia*) between 10.00 and 16.00 P.M. (Ny-Ålesund local time). CO₂ assimilation rates (*A*) and stomatal conductance (*g_s*) were measured using a portable infrared gas analyzer system LI-6400XT (Li-Cor, Lincoln, NE, USA) by clamping the single leaves (or composite leaves, depending on the species) into a 2 cm² LI-6400-40 leaf chamber. For rapid measurements, leaves inside the cuvette were exposed to ambient CO₂ concentration (390 $\mu\text{mol mol}^{-1}$, *C_a*), relative humidity was maintained

between 40 and 60 %, and air temperature was maintained around 10 °C. The latter value was chosen because, in preliminary measurements carried out at the site, it was shown to be the optimum temperature for assimilation for all species analyzed. During the entire set of measurements, the VPD values recorded were between 0.3 and 0.6 kPa, excluding any negative effect on the stomatal conductance or assimilation rates. Light was provided by a LED system integrated in the chamber, and the measurements were taken at 1000 $\mu\text{mol photons m}^{-2} \text{s}^{-1}$ intensity (photosynthetic photon flux density, PPDF). This value was selected from previous measurements carried out at the site since it was the optimum light conditions for photosynthesis regarding the plant species analyzed.

Response curves of A to different light intensities were generated with PPDF values ranging between 0 and 2000 $\mu\text{mol photons m}^{-2} \text{s}^{-1}$ in the following order: 1000, 0, 30, 60, 120, 400, 700, 1000, 1300, 1700 and 2000. For these measurements, the CO_2 concentration was fixed at 390 $\mu\text{mol mol}^{-1}$ and air temperature at 10 °C. From these light curves, the values of maximum assimilation rate (A_{max}) were calculated following Bernacchi et al. (2003).

Response curves of A to different CO_2 concentrations were generated by changing the C_a values inside the cuvette, ranging between 0 and 2000 $\mu\text{mol mol}^{-1}$ in the following order: 390, 0, 30, 60, 120, 250, 390, 650, 1300, 1700, 2000, using a CO_2 mixer. The PPDF intensity was set to 1000 $\mu\text{mol photons m}^{-2} \text{s}^{-1}$ and the temperature to 10 °C. Measurements at each step were recorded after equilibration to a steady state, and leaking tests were performed. One key parameter in Farquhar-type photosynthesis models, the maximum rate of Rubisco carboxylase activity ($V_{c,\text{max}}$), was calculated following Farquhar et al. (1989). This represents the slope of the first linear part of the $A-C_i$ curve, normally including the first 5–7 points of the $A-C_i$ curve (Long and Bernacchi 2003).

The dependence of assimilation rate on leaf temperature was studied by adapting the leaf to different temperatures. This was performed by exposing for about 15 min the leaf in the cuvette to the following series of temperatures: 10, 15, 25 and 10 °C. At each temperature value, measurement of A was performed at 3 light intensities 200, 500 and 1000 $\mu\text{mol photons m}^{-2} \text{s}^{-1}$. The 200 and the 1000 $\mu\text{mol photons m}^{-2} \text{s}^{-1}$ values represent the limiting and the optimum light intensities, respectively, as verified in preliminary measurements, while 500 $\mu\text{mol photons m}^{-2} \text{s}^{-1}$ were chosen as an intermediate light intensity. These measurements were performed at 390 $\mu\text{mol mol}^{-1} \text{CO}_2$.

Carbon isotope composition analysis

During the 2013 campaign, plant material for carbon isotope composition analysis was harvested at the end of the

gas exchange measurement period (12th July). Fresh plant material was separated into above- and below-ground elements and dried in an oven at 70 °C for 48 h. The above-ground material was, for all species except *S. polaris* separated into “new” material (considered as the biomass formed in the current season) and “old” material (considered as the biomass formed during the previous season). After grinding, dry material was processed using an elemental analyzer (model NA 1500, Carlo Erba, Milan, I), coupled with a continuous flow mass spectrometer (model ISOPRIME). The $\delta^{13}\text{C}$ was calculated with respect to a standard [Pee Dee Belemnite (PDB)], as:

$$\delta^{13}\text{C}_{\text{sample}} = (R_{\text{sample}} - R_{\text{st}})/R_{\text{sample}},$$

where R is the isotope ratio of carbon ($^{13}\text{C}/^{12}\text{C}$) measured by isotope ratio mass spectrometry.

The Δ value is calculated as:

$$\Delta = (\delta^{13}\text{C}_{\text{CO}_2} - \delta^{13}\text{C}_{\text{sample}})/(1 + \delta^{13}\text{C}_{\text{sample}})$$

where $\delta^{13}\text{C}_{\text{CO}_2}$ is the carbon isotope composition of the atmospheric CO_2 .

Laboratory analyses

To limit disruptive impacts on natural vegetation, only one sample of phytomass (230 mm diameter) was collected for each analyzed vegetation type. Soil samples were collected at two different depths (0–4; 5–10 cm) per plot for each vegetation type. To determine dry phytomass and water content in the soil, each sample was weighed, oven dried at 105 °C for 24 h and then re-weighed. For each sample, the above-ground and below-ground phytomass were separated. The soil samples (sieved <2 mm) were analyzed for total organic matter (TOM) lost on sample ignition (Nelson and Sommers 1996).

Data analyses

Multiple regression models are used to analyze the relationship between a dependent variable and one or more continuous independent variables, while general regression models are used when the design includes both continuous and categorical independent variables. Backward stepwise regression commences the analysis, initially including all continuous and categorical variables, and then variables are successively deleted if that leads to improvement in the model until the best fit of the model is achieved.

The influence of the different environmental factors (soil temperature, soil moisture and PAR as continuous variables; time and vegetation community as categorical variables) on CO_2 fluxes measured at the plot scale was assessed separately for NEE and ER using a general

regression model (GRM) selecting the significant factors by the backward stepwise method both at (1) intra-community level (e.g., within each vegetation community) and at (2) inter-community level (e.g., among different vegetation communities). The influence of the species-specific photosynthetic performances (A , $V_{c,max}$), and of LAI on the CO_2 fluxes measured at plot scale was tested by GRM. GRM was performed using the software Statistica®.

Daily and seasonal means ($\pm SE$) of soil temperature, soil moisture, PAR, NEE, ER were computed using the software Statistica®. For the calculation of daily means, we used all the measurements carried out during a specific day for each plot and parameter. For the seasonal means, we used all the records performed during each day of measurement over the entire selected period.

Data on photosynthetic performance are presented as mean $\pm SE$. Before performing the ANOVA test, the Shapiro–Wilk test of normality was undertaken to determine whether the data in each group were normally distributed. All statistical analyses were conducted using Sigma Plot v.12.5 (Systat Inc., San Jose, CA, USA).

Results

Field measurements: site characterization

At the CCT site, the soils exhibited different physical and chemical characteristics (grain size, % water content, pH, % soil total organic matter) in relation to the different vegetation communities (Table 1). All soils showed low pH (ranging from 4.7 to 5.7) and relatively high soil total organic matter content (ranging from 23 % under *S. oppositifolia* to 38 % under *C. tetragona*). The phytomass (dry weight) was highest for *C. tetragona* and lowest for *D. octopetala*, while the water content of the phytomass ranged from 12 % (*C. tetragona*) to 37.3 % (*S. polaris*) (Table 1).

Despite their similar topographic features, soil temperature and soil moisture measured at 2 cm depth changed in relation with the selected community type (Fig. 1). The lowest soil temperature (6.3 °C) and the highest soil moisture (50 %) were measured under the snowbed

community dominated by *S. polaris*, while the highest soil temperature (8.2 °C) and lowest soil moisture characterized the dwarf shrub *D. octopetala*.

CO₂ fluxes at the plot scale

Comparing the seasonal means of NEE and ER in the two transition seasons (EGS in 2012, Fig. 2a, vs. BGS in 2013, Fig. 2b), each vegetation community exhibited different values and trends. At the EGS (2012), only *D. octopetala* showed negative NEE (indicating CO_2 uptake from the atmosphere), and *S. polaris* and *S. oppositifolia* had NEE values close to zero (neither uptake, nor release), while *C. tetragona* and *C. rupestris* were characterized by positive NEE (indicating CO_2 release to the atmosphere) (Fig. 2a). The seasonal means of NEE at the BGS in the following year (2013) were positive for all the vegetation communities (Fig. 2b), with the highest release of CO_2 to the atmosphere measured for *C. tetragona* and *C. rupestris*, and the lowest for *D. octopetala*.

The patterns of seasonal means of NEE among the different vegetation communities were similar in the measurements carried out in two different sites (CCT and SND) in 2012 (Online Resource 1). Similar patterns between the communities were also observed in the 2013 measurements at the CCT site (Fig. 2b), although with different absolute values.

In contrast, the patterns of seasonal mean of ER among vegetation communities at the CCT site were opposite when comparing the EGS period (2012, Fig. 2a) with the BGS (2013, Fig. 2b). In 2012, *C. tetragona* exhibited the lowest ER and *D. octopetala* the highest, but in 2013 these patterns were reversed. The vegetation community patterns of mean seasonal ER identified at the BGS (2013) reflected the gradient of soil total organic matter measured in the upper part of the soils (0–4 cm), excepting that of *S. oppositifolia* (Table 1).

Mean seasonal NEE and ER did not provide information on their changes during the growing season.

Mean daily NEE in 2013 showed positive values for most communities and for all the periods of measurement, with the exception of *D. octopetala*, which started to record CO_2 uptake only after the completion of

Table 1 Soil characteristics [water content (WC), % soil total organic matter (TOM), pH at 0–4 cm depth], phytomass [dry weight (DW) and water content] of the five vegetation plot types

Plot type	Soil WC (%)	TOM (%)	pH	Phytomass DW (g)	Phytomass WC (%)
<i>C. tetragona</i>	7.2	38	5.3	54.7	12.4
<i>D. octopetala</i>	27.9	30.6	5.3	20	19.6
<i>S. polaris</i>	36.9	30.3	4.7	22	37.3
<i>C. rupestris</i>	38.8	32.2	ND	24.8	29.5
<i>S. oppositifolia</i>	37.1	23.5	5.7	22	31.4

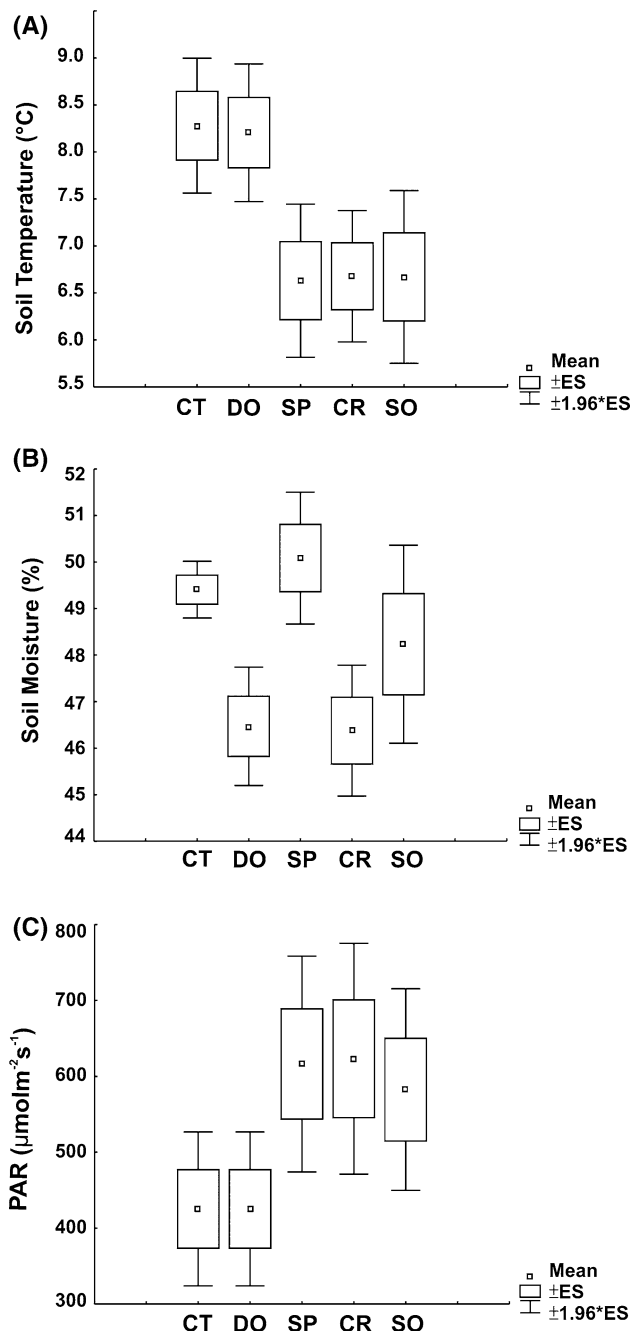


Fig. 1 Mean seasonal values of soil temperature (°C), gravimetric water content (%), PAR ($\mu\text{mol m}^{-2} \text{s}^{-1}$) of the five selected vegetation communities/target species analyzed at the plot scale at the CCT site in 2013. Values represent mean \pm SE ± 1.96 SE (SE = standard error). CT = *C. tetragona*; DO = *D. octopetala*; SP = *S. polaris*; CR = *C. rupestris*; SO = *S. oppositifolia*

unfolding of new leaves (arrow in Fig. 3b), and of *S. polaris*, similarly only showed uptake after producing the new leaves later than *D. octopetala* (Fig. 3c, left panel). For all vegetation communities, ER increased progressively throughout the growing season (Fig. 3a–e, left panels).

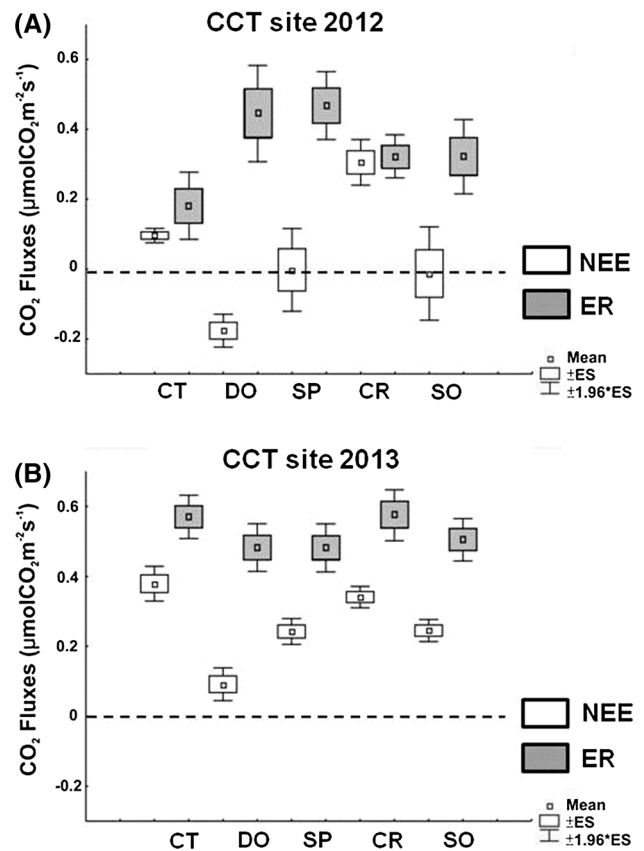


Fig. 2 Seasonal means of Net ecosystem exchange (NEE, $\mu\text{mol CO}_2 \text{ m}^{-2} \text{ s}^{-1}$, white rectangle) and ecosystem respiration (ER, $\mu\text{mol CO}_2 \text{ m}^{-2} \text{ s}^{-1}$, gray rectangle) measured at the plot scale for the 5 selected vegetation types at the CCT site. **a** 2012 after the peak of the growing season (1st–15th August 2012); **b** 2013: at the beginning of the growing season (June 7– July 10, 2013). Values represent mean (\pm SE ± 1.96 SE) (SE = standard error). CT = *C. tetragona*; DO = *D. octopetala*; SP = *S. polaris*; CR = *C. rupestris*; SO = *S. oppositifolia*

Cumulative NEE showed that all vegetation communities acted as sources releasing CO_2 , although with different patterns (Fig. 3a–e, right panels). Cumulative NEE tended to decrease with time (switching from CO_2 source to sink) for *D. octopetala*, while it flattened (but did not decrease) for *C. tetragona*, *S. polaris* and *S. oppositifolia*. Only the grass *C. rupestris* exhibited a continued increase in cumulative NEE in mid-July (Fig. 3d). *D. octopetala* was characterized by the lowest cumulative NEE (although still >0), while *C. rupestris* showed the highest. Cumulative NEE exhibited very similar values across *C. tetragona*, *S. polaris* and *S. oppositifolia* (Fig. 3a–e, right panels). Cumulative ER was characterized by different patterns among the studied vegetation. *C. rupestris* showed the highest ER and *C. tetragona* the lowest, while the other vegetation communities exhibited similar values (Fig. 3). The main factors affecting NEE at inter-community level differed between the two transition seasons (EGS in 2012 vs. BGS in 2013).

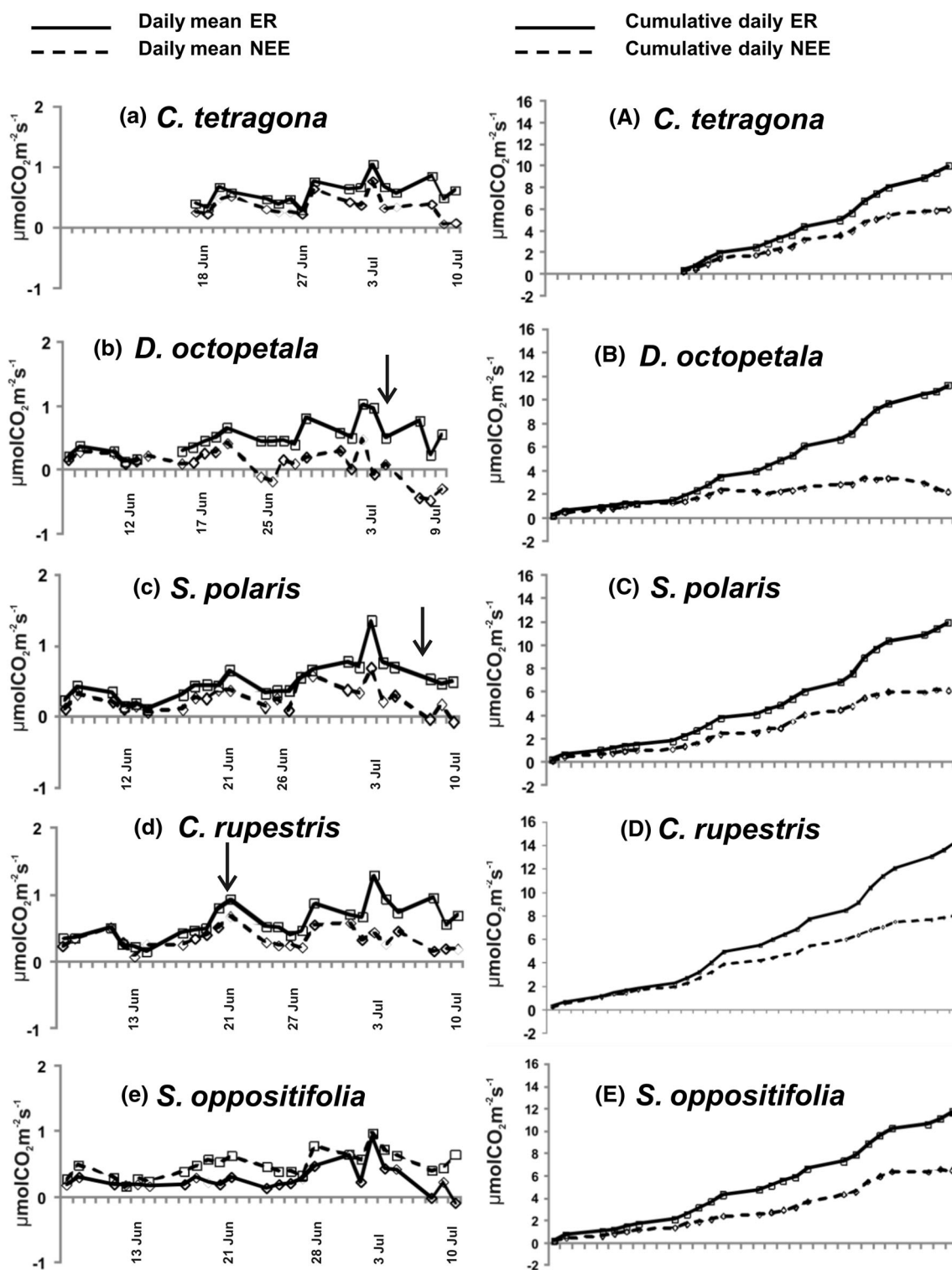


Fig. 3 Mean daily (left panels) and cumulative daily (right panels) NEE (black dashed line) and ER (black solid line) of the selected vegetation communities in 2013: *C. tetragona* (a, A); *D. octopetala*

(b, B); *S. polaris* (c, C); *C. rupestris* (d, D); *S. oppositifolia* (e, E). Measurements started on June 7, 2013, and ended on July 10, 2013. On x-axis, each point represents a single day

At the EGS (2012), the most important factors affecting NEE were plot type and PAR, while at the BGS (2013) the factors were soil temperature followed by date and plot type

(Table 2). Soil temperature was the most important factor affecting ER at the BGS (2013), with soil moisture and plot type having a statistically significant but less important influence.

At intra-community level, we focused on the 2013 data and on the five selected vegetation communities. The daily means of NEE, ER and of the main abiotic environmental factors measured in 2012 at the CCT site are presented in Online Resources 2 and 3. Soil temperature was the most important factor influencing NEE for all the vegetation communities, followed by date (Table 3). Soil moisture was secondary significant but less important factor for *C. rupestris*, *S. oppositifolia* and *S. polaris*, while the other factors exerted a limited influence (Table 3). It is notable that PAR was not among the driving factors of NEE, despite the differences observed among the different vegetation communities (Fig. 1). Soil temperature was the key factor affecting ER for all the communities (Table 3), while soil moisture played a minor influence and only for *S. polaris* and *D. octopetala*.

Photosynthetic capacity

The photosynthetic parameters of the different species both from rapid direct measurements and extrapolated from CO₂ and light curves are given in Table 4. Leaves of *S. polaris* and *D. octopetala* exhibited the highest assimilation rates, while *S. oppositifolia* showed the lowest. The high value of *A* in *D. octopetala* is consistent with the high stomatal conductance (*g_s*) recorded for this species. The low stomatal conductance of *S. oppositifolia* is, likewise, consistent with it having the lowest value of *A* and *g_s* (Table 4). These patterns also resemble the measured nitrogen content in leaves (Table 4), which was lowest in *S. oppositifolia*. The assimilation rates measured at increasing atmospheric CO₂ concentration (*A–C_i* curve), at constant light of

1000 μmol m⁻² s⁻¹ and a temperature of 10 °C, are shown in the upper panel of Fig. 4. The four studied species showed similar behavior, with similar trends in the initial part of the curve (from 0 to 300 μmol mol⁻¹ CO₂) as well as in the latter part of the curve, when *A* is usually saturated. Although all species reached high values of *A* (ranging between 15 and 20 μmol m⁻² s⁻¹), none showed a clear saturation of *A* to increasing CO₂ concentration. The lack of significant differences in photosynthetic parameters was confirmed by the values of *V_{c,max}* calculated from the *A–C_i* curves (Table 4), with *D. octopetala* exhibiting the highest *V_{c,max}*, and *S. oppositifolia* the lowest values, although these differences were not statistically significant (Table 4).

The CO₂ assimilation rate measured at different light intensities showed significant differences among species (Fig. 4, lower panel; Table 4). Independent of light intensity, *S. oppositifolia* exhibited the lowest *A* values, while *D. octopetala* and *S. polaris* always exhibited the highest values although, at saturating light levels (between 1000 and 2000 μmol m⁻² s⁻¹). These differences were shown when considering the values of *A_{max}*, calculated from the light curves (Table 4). *C. rupestris* showed similar values at saturating light intensities, but intermediate values of *A* below 1000 μmol m⁻² s⁻¹ (Fig. 4, lower panel).

Concerning the dependence of the assimilation rates from leaf temperature at each different light intensity (200, 500 and 1000 μmol m⁻² s⁻¹, respectively), all species analyzed were characterized by a clear decrease in *A* at increasing leaf temperatures, although with species-specific patterns (Fig. 5). *S. polaris* leaves showed a strong decrease in assimilation rates from 15 to 25 °C, whereas in

Table 2 Effect of plot (vegetation community) and abiotic factors (soil temperature, soil moisture, PAR, date, time) on NEE and ER in 2012 and 2013 at inter-community level close to the climate change tower (CCT) at Ny Ålesund, as tested by general regression models, using backward stepwise method of selection of the variables

	<i>N</i> = 114	<i>F</i>	<i>p</i>	<i>R</i>	<i>N</i> = 537	<i>F</i>	<i>p</i>	<i>R</i>
NEE inter-plot 2012					NEE inter-plot 2013			
Intercept		7.3	<0.001		Intercept	96.04	0	
PAR		4	<0.05		PAR	10.82	<0.001	
<i>T</i>					<i>T</i>	219.42	0	
% Moist					% Moist	15.82	<0.001	
Date					Date	96.17	0	
Time					Time			
Plot		5.7	<0.001		Plot	51.22	0	
Full model		5.4	<0.001	0.36	Full model	56.9	<0.001	0.68
ER inter-plot 2012					ER inter-plot 2013			
Date					Date			
Time					Time			
<i>T</i>					<i>T</i>	444	<0.001	
% Moist					%Moist	15.4	<0.001	
Plot					Plot	10.4	<0.001	
Full model			>0.05		Full model	78.4	<0.001	0.83

Values are reported only for statistically significant effects

Table 3 Effect of abiotic factors (soil temperature, soil moisture, PAR, date, time) on NEE and ER at intra-community level in 2013 close to the climate change tower (CCT) at Ny Ålesund, as tested by general regression models, using backward stepwise method of selection of the variables

	NEE			ER		
	<i>F</i>	<i>P</i>	<i>R</i>	<i>F</i>	<i>P</i>	<i>R</i>
	<i>C. tetragona</i> (n = 68)			<i>C. tetragona</i> (n = 32)		
PAR ($\mu\text{mol m}^{-2} \text{s}^{-1}$)						
Soil temperature ($^{\circ}\text{C}$)	97	<0.001		35.7		
Soil moisture (%)						
Date	23	<0.001				
Time						
Full model	99.3	<0.001	0.86	35.7	<0.001	35.7
	<i>D. octopetala</i> (n = 99)			<i>D. octopetala</i> (n = 43)		
PAR ($\mu\text{mol m}^{-2} \text{s}^{-1}$)	6.6	<0.001				
Soil temperature ($^{\circ}\text{C}$)	33.5	<0.001		146.7	0.001	
Soil moisture (%)				29	<0.001	
Date	63.3	<0.001				
Time				6	<0.001	
Phenology						
Full model	23.8	<0.001	0.67	57.7	<0.001	0.9
	<i>S. polaris</i> (n = 117)			<i>S. polaris</i> (n = 51)		
PAR ($\mu\text{mol m}^{-2} \text{s}^{-1}$)						
Soil temperature ($^{\circ}\text{C}$)	59.2	<0.001		1273	<0.001	
Soil moisture (%)	10.6	<0.001		7.5	<0.001	
Date	29.9	<0.001				
Time						
Phenology						
Full model	21.7	<0.001	0.61	64.7	<0.001	0.85
	<i>C. rupestris</i> (n = 123)			<i>C. rupestris</i> (n = 32)		
PAR ($\mu\text{mol m}^{-2} \text{s}^{-1}$)	8.9	<0.001				
Soil temperature ($^{\circ}\text{C}$)	21.9	<0.001		285	<0.001	
Soil moisture (%)	6.8	0.001				
Date	12.4	<0.001				
Time						
Phenology	6.1	<0.001				
Full model	8.6	<0.001	0.56	285.9	<0.001	0.93
	<i>Saxifraga oppositifolia</i> (n = 120)			<i>Saxifraga oppositifolia</i> (n = 50)		
PAR ($\mu\text{mol m}^{-2} \text{s}^{-1}$)						
Soil temperature ($^{\circ}\text{C}$)	38.1	<0.001		44.4	<0.001	
Soil moisture (%)	6.2	<0.001				
Date						
Time						
Phenology	7.4	<0.001				
Full model	14	<0.001	0.58	44.4	<0.001	0.69

Values are reported only for statistically significant effects. For *C. tetragona*, phenology was not inserted as a factor because there were no apparent different phenological stages

D. octopetala the decrease occurred from 10 to 15 $^{\circ}\text{C}$. Notably, in *S. oppositifolia* a light intensity of 200 $\mu\text{mol m}^{-2} \text{s}^{-1}$ was not sufficient to maintain positive assimilation rates even at optimal temperatures for this species (10 $^{\circ}\text{C}$).

Role of species-specific photosynthetic capacity in CO_2 fluxes measured at the plot scale

As the four species selected for the measurements at the leaf scale exhibited significant and species-specific

Table 4 Assimilation rate (A) and stomatal conductance (g_s) measured at $1000 \mu\text{mol m}^{-2} \text{s}^{-1}$, 10°C and 390ppm

Species	A ($\mu\text{mol m}^{-2} \text{s}^{-1}$)	g_s ($\text{mol m}^{-2} \text{s}^{-1}$)	$V_{c,\text{max}}$ ($\mu\text{mol m}^{-2} \text{s}^{-1}$)	A_{max} ($\mu\text{mol m}^{-2} \text{s}^{-1}$)	Leaf (N %)	LAI	Leaf carbon isotope discrimination (Δ) (‰)
<i>D. octopetala</i>	$4.65^{\text{ab}} \pm 0.48$	$0.361^{\text{a}} \pm 0.063$	89.41 ± 16.94	$4.67^{\text{a}} \pm 0.29$	$1.895^{\text{b}} \pm 0.055$	0.7	$22.198^{\text{a}} \pm 0.164$
<i>S. polaris</i>	$5.11^{\text{a}} \pm 0.75$	$0.125^{\text{bc}} \pm 0.018$	66.57 ± 8.94	$4.16^{\text{ab}} \pm 0.67$	$2.842^{\text{a}} \pm 0.068$	0.4	$19.866^{\text{c}} \pm 0.251$
<i>C. rupestris</i>	$3.16^{\text{bc}} \pm 0.30$	$0.201^{\text{ab}} \pm 0.027$	67.81 ± 12.65	$4.46^{\text{a}} \pm 0.69$	$2.520^{\text{ab}} \pm 0.048$	0.3	$21.495^{\text{ab}} \pm 0.162$
<i>S. oppositifolia</i>	$2.33^{\text{c}} \pm 0.16$	$0.058^{\text{c}} \pm 0.018$	55.82 ± 2.73	$2.80^{\text{b}} \pm 0.49$	$1.255^{\text{b}} \pm 0.171$	0.6	$20.825^{\text{bc}} \pm 0.395$

^a, ^b, ^c indicates the results of the Shapiro–Wilk test of normality ($p < 0.05$)

Maximum rate of Rubisco carboxylase activity ($V_{c,\text{max}}$) and light-saturated photosynthetic rate (A_{max}) calculated from $A-C_i$ and A -light curves, respectively. Leaf nitrogen content and leaf carbon isotope discrimination (Δ) measured on phytomass harvested in July 2013. Leaf area index (LAI) measured in 2012, after the completion of leaf development. Values are mean \pm SE ($n = 5$)

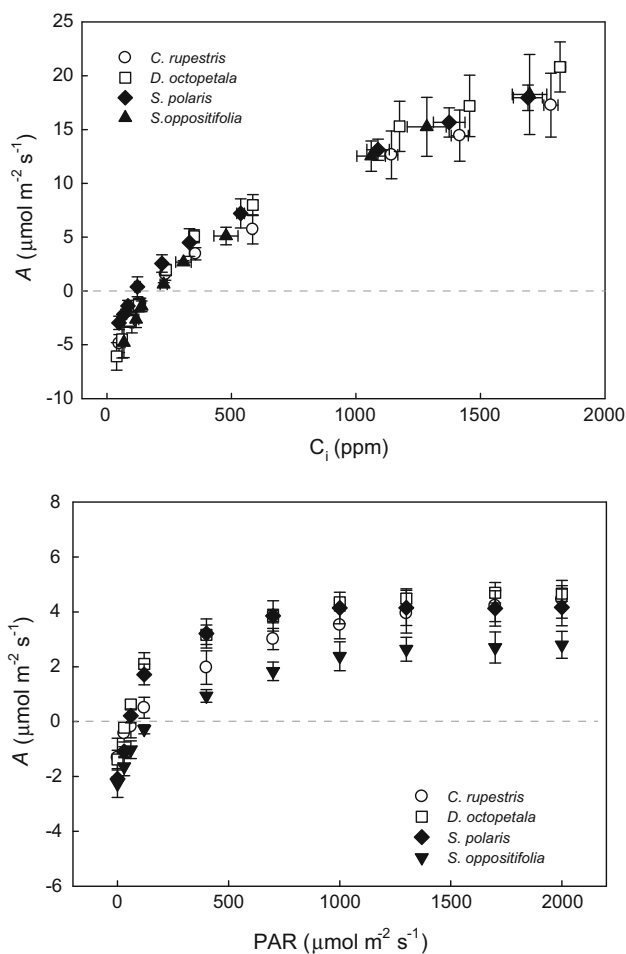


Fig. 4 CO_2 concentration (C_i) dependence of assimilation rates (A) (upper panel), and light intensity dependence of assimilation rates (A) (lower panel) at the leaf level for the four target species, (values are mean \pm SE, $n = 4$)

differences in their photosynthetic capacities, we used GRM to test their influence on NEE (as GEP directly influences NEE) measured in 2013 (excluding the data of the *C. tetragona* plot), to assess whether they also influence the overall CO_2 fluxes measured at the plot scale. Soil

temperature remained the most important factor, followed by $V_{c,\text{max}}$, date, and A_{max} , while soil moisture and PAR exerted only a very limited influence on NEE at the plot level (and also at inter-community level) (2013 data) (Table 5, left side). These data indicate the importance of species-specific photosynthetic capacities in influencing NEE.

As LAI can also be a very important factor affecting NEE, we performed a separate GRM including it as biotic factor. This analysis (Table 5, right side) showed that the two most important factors influencing NEE were soil temperature and LAI, followed by date and leaf nitrogen.

Isotopic characteristics

All species considered are perennial vascular plants and dicotyledons (except *C. rupestris*, which is a monocot). *D. octopetala*, *C. rupestris*, *S. oppositifolia* plants possessed, at the time of the measurements, a green (“new”) above-ground element, developed during the season of the measurements, and a brown (“old”) above-ground element, developed during the previous season. *S. polaris* possessed only green leaves developed in the current season. The values of carbon isotope composition ($\delta^{13}\text{C}$) measured on above- and below-ground parts of the plants were characteristic of C_3 photosynthetic pathway, which is expected in Arctic regions (Billing, 1987). The $\delta^{13}\text{C}$ value varied between -28 and -31 ‰ in the above-ground dry matter, and it was about -29 ‰ in below-ground matter (data not shown). The species studied also showed variations in carbon isotope discrimination (Δ), reflecting differences in the ratio C_i/C_a integrated over the period of development of the plant material analyzed, in the case of the green (“new”) above-ground element developed in the 2013 growing season. The Δ values of green (“new”) above-ground matter (Table 4) varied from 19.9 ‰ in *S. polaris* to 22.2 ‰ in *D. octopetala*, indicating higher photosynthetic activity in the latter. While the Δ values of the

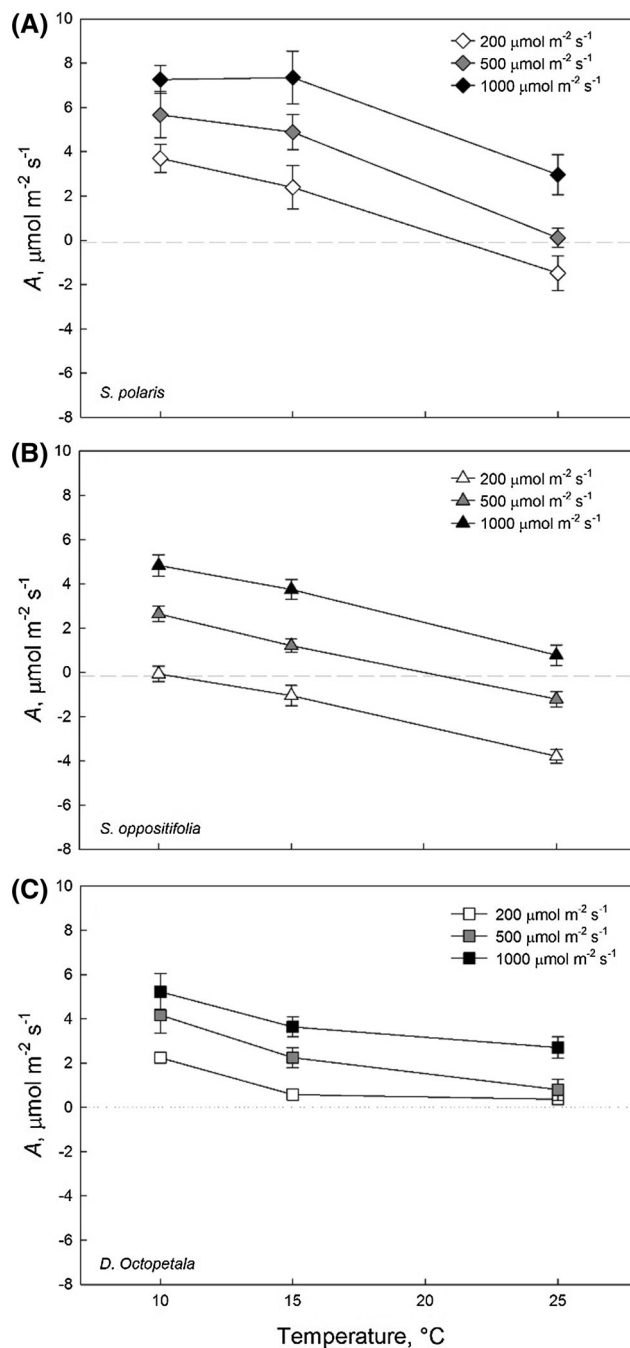


Fig. 5 Temperature dependence of assimilation rates (A) in *D. octopetala* (a), *S. polaris* (b), and *S. oppositifolia* (c) at different light intensities: 200 (white symbols), 500 (gray symbols) and 1000 $\mu\text{mol m}^{-2} \text{s}^{-1}$ (black symbols) (values are mean \pm SE, $n = 4$)

previous season's above-ground material in *D. octopetala* (22.2 ‰) were comparable with those of the "new" season's above-ground element, in *C. rupestris* and *S. oppositifolia*, the Δ values of "old" above-ground matter were slightly lower (20.9 and 20.2 ‰, respectively) than those of the "new" above-ground matter (developed in the current season). The Δ values in below-ground matter did

not show significant differences across species and ranged from 20.5 to 20.9 ‰.

Discussion

Site characteristics

Our study site is characterized by vegetation and soil conditions typical and representative of a High Arctic tundra in mesic-xeric conditions. The spatial distribution of our target species reflects the local soil moisture gradient (Fig. 1b). The extremes of this gradient are represented by *D. octopetala* and *S. polaris*, the former in the drier conditions, the latter in wetter conditions (Sjögerstern et al. 2006). These species also represent the two extremes of the soil temperature gradient of our study site (Fig. 1).

Measured soil total organic matter varied with the overlaying plant species (Table 1), consistent with the findings of Muraoka et al. (2008). In particular, higher values were observed under *S. polaris* and *D. octopetala* than under *S. oppositifolia*. Leaf N content reflected with the nutrient content of the soils under each plant species (Tables 1, 4).

CO₂ fluxes at the plot scale

The NEE and ER values found in our study differed between vegetation communities, in agreement with previous studies of tundra vegetation in Svalbard (Lloyd 2001; Sjögerstern et al. 2006; Elberling 2007), and elsewhere in the Arctic (Welker et al. 2004; Oberbauer et al. 2007).

Mean seasonal NEE and cumulative NEE values (Figs. 2, 3) support the conclusion that all communities released CO₂ (i.e., acted as "CO₂ sources") in both transition seasons.

During the BGS, the release was due to the high ER associated with increasing soil temperatures and release of CO₂ from the thawing soil, as described by Groendahl et al. (2007). The release at the EGS may reflect the larger decrease in GEP (up to 95–100 %) compared to ER, with ER becoming dominant in shaping NEE, as described by Christiansen et al. (2012).

At our study site, the CO₂ release was higher at the BGS than at the EGS (Fig. 2). This may indicate the occurrence of pulse periods with significant primary production at the EGS. Christiansen et al. (2012) also recorded a GEP significantly different from 0 in October at sub-zero temperatures in the High Arctic. CO₂ release could also be the prevalent process occurring at the BGS during the snow-melt period, before the completion of leaf development (Uchida et al. 2010).

Table 5 Effect of biotic (species-specific photosynthetic characteristics— A , $V_{c,max}$, and species phenology—as categorical factor) without LAI (left side of the table) and with LAI (right side of the table) and of abiotic factors (soil temperature, soil moisture, PAR,

date, time) on NEE at the beginning of the growing season in 2013 at inter-community level close to the climate change tower (CCT) at Ny Ålesund, as tested by general regression models, with backward stepwise method of selection of the variables

NEE							
Factors	F	p	R	Factors	F	p	R
A_{max}	53.7	<0.001		A_{max}	NS		
$V_{c,max}$	95.2	<0.001		$V_{c,max}$	NS		
$N\%$	19.4	<0.001		$N\%$	30	<0.001	
PAR	12.8	<0.001		PAR	12.8	<0.001	
T	147.2	<0.001		T	148	<0.001	
Moist %	14.5	<0.001		Moist %	17	<0.001	
Date	78.1	<0.001		Date	78.1	<0.001	
Time	NS			Time	NS		
Phenology	NS			Phenology	NS		
				LAI	141.4	<0.001	
Full model	42.8	<0.001	0.64	Full model	50	<0.001	0.64

NS not statistically significant

Values are reported only for statistically significant effects. *C. tetragona* was excluded from this analysis as the photosynthetic characteristics of this species were not measured due to logistical constraints

Our data show that GEP (calculated as the difference between NEE and ER) follows species-specific patterns (Fig. 2). The deciduous shrubs (*D. octopetala* and *S. polaris*) exhibited a larger GEP at the EGS, as might be expected of deciduous species, whose GEP is very low at the BGS and increases throughout the development of the vegetative stages. The evergreen shrub (*C. tetragona*) and the grass (*C. rupestris*) showed the opposite pattern, with higher GEP at the BGS, as they are either already photosynthetically active (*C. tetragona*), or are able to develop rapidly their new leaves (*C. rupestris*). The evergreen forb *S. oppositifolia* exhibited similar GEP both at the BGS and at the EGS, and, for this species, the different NEE was due to changes in ER.

The patterns of mean daily NEE and of cumulative NEE (Fig. 3) allow some evaluation of the role of phenology, although in our data its influence was not statistically significant for all the selected target species (Tables 3, 5). In particular, leaf development and unfolding in the early part of July 2013 coincided with a switch from positive to negative NEE values (i.e., from CO₂ source to sink) for the deciduous *D. octopetala* and *S. polaris*. These data confirm similar observations carried out on *S. polaris* (Uchida et al. 2010), *D. octopetala* and other High Arctic tundra species (Euskirchen et al. 2012) and emphasize the importance of seasonal factors, with particular reference to snowmelt and vegetative phenological stages (e.g., leaf development and unfolding) in influencing the patterns of NEE at the BGS. According to Groendahl et al. (2007), the greening period (when the development of the vegetative phenological stages is completed) coincides with the strongest sink strength of Arctic ecosystems.

At inter-community level, the biotic and abiotic factors influencing NEE changed comparing the EGS (2012) with the BGS (2013) (Table 2) emphasizing the need to analyze in detail and compare these two transition seasons (Lüers et al. 2014). Plot type (as generic categorical factor) and PAR were the most important factors at the EGS, emphasizing the importance of species-specific responses (Fig. 2). In 2013, BGS soil temperature was the most important factor, followed by date and plot type. There is a large degree of inter-annual variability in tundra NEE as climatic factors may vary widely from year to year (Lafleur and Humphreys 2008; Lund et al. 2010; Euskirchen et al. 2012), and it is thus unsurprising that the factors affecting NEE could differ throughout and between years.

Soil temperature was the key factor affecting ER for all vegetation types, as previously reported by Elberling (2007) at a different location on Svalbard. In the current study, soil moisture did not influence ER, probably because the study site is characterized by relatively well-drained soil conditions. The observation that the plots studied at this study site are mainly CO₂ sources is consistent with the hypothesis that relatively dry or well-drained areas are likely to be weaker sinks or even CO₂ sources (McFadden et al. 2003; Welker et al. 2004; Sjögerstern et al. 2006).

Photosynthetic capacity and isotope characteristics

Assimilation rates (A) show species-specific patterns (Table 4), resembling the measured nitrogen content in leaves (Table 4). Our light-curve results are similar to those obtained by Muraoka et al. (2008) and confirm the

occurrence of different light-saturated photosynthesis rates (A_{\max}) between the species. This may be explained by differences in light harvesting and light utilization efficiency related to structure and composition of the photosynthetic apparatus. Further study of pigment composition of the photosynthetic apparatus may clarify these differences in light utilization. The lack of saturation of the assimilation curve in response to increasing CO_2 concentration ($A-C_i$) possibly indicates a high ribulose phosphate regeneration capacity (Farquhar et al. 1980) and is relevant to consideration of responses to future increases in atmospheric CO_2 concentration (Norby and Luo 2004; Nowak et al. 2004). The clear decrease in A at increasing leaf temperatures indicates adaptation of these species to cold temperatures and may provide an indications on potential vulnerability of these species to a warmer climate, with *S. polaris* being potentially less challenged than *D. octopetala* or *S. oppositifolia*. The issues related to the species-specific adaptation to low temperatures are worth of further investigations as could trigger significant feedbacks in a climate change context.

The carbon isotope composition ($\delta^{13}\text{C}$) of the four species studied confirms that they are C_3 species. Leaf carbon isotope discrimination (Δ) on “new” above-ground dry matter showed significant differences between species, indicating higher photosynthetic activity in *D. octopetala*, over the entire period of leaf viability compared to other species. This is consistent with the species-specific differences and patterns identified in the analyses of photosynthetic capacities. The Δ values of the above-ground biomass between the current and past season indicate different patterns across species. While the deciduous *D. octopetala* had comparable values, *C. rupestris* and *S. oppositifolia* showed lower values for the past season, which may indicate a higher level of photosynthesis in the 2013 season compared to 2012. These differences could also indicate the occurrence of post-photosynthetic carbon fractionation (Brüggemann et al. 2011, and references therein) during respiration.

This type of isotope fractionation needs to be further investigated in Arctic species, with the aim to use the isotope approach, together with the gas exchange approach as tool to monitoring Carbon fluxes in Arctic regions.

Role of species-specific photosynthetic capacities in CO_2 fluxes measured at the plot scale

LAI has been identified as one of the most important biotic factors explaining the majority of NEE variance in Arctic and sub-Arctic environments (Shaver et al. 2013) as also noted here. Considering the role of photosynthetic capacities separately, our data indicate that species-specific photosynthetic capacities are key biotic factors affecting

NEE at inter-community level (Table 5). Their use, rather than the generic categorical factor “plot type,” provides clearer understanding of the NEE patterns observed among the selected target species.

Considering the species-specific mean seasonal NEE across *S. oppositifolia*, *S. polaris* and *D. octopetala*, there was an increasing sink effect apparent with increasing successional status. Muraoka et al. (2008) made similar observations and linked these differences to differing soil nutrient availability, photosynthetic capacity and biomass distribution. *S. polaris* is a dominant species in the late successional stages of communities in deglaciated areas and is rarely present in the early stages of community development, which are dominated by *S. oppositifolia* (Nakatsubo et al. 2010).

Dryas octopetala exhibited the lowest NEE and largest GEP, in agreement with its highest $V_{c,\max}$ and LAI. This species was also characterized by the highest soil temperature and lowest soil moisture and, probably, by the earliest snowmelt and longest growing season, all of which would contribute to explaining its NEE and GEP (Sjögerstern et al. 2006; Muraoka et al. 2008). The higher photosynthetic rates recorded for *D. octopetala* are also in agreement with the findings of Bartak et al. (2012).

Measurement of CO_2 fluxes performed at different spatial scales (from leaf to plot) demonstrated that spatial variation in CO_2 fluxes is influenced by both biotic and abiotic factors. Among the biotic factors, our data emphasize the importance of species-specific photosynthetic capacities, coupled with phenological stage and LAI. Among the abiotic factors, temperature is crucial in affecting ER and, in most cases, NEE, as well as in shaping photosynthetic performances in some species.

Our data highlight the need to understand and quantify the ecological role of dominant species in natural communities and their contribution to the C cycle (as sinks or sources). Potential changes of vegetation characteristics in response to climate change (e.g., community composition, dominance, life form, species phenology) may trigger significant feedbacks on ecosystems and to the climate system. Due to the heterogeneity typical of Arctic tundra, the effect of climate change on CO_2 uptake/release will vary strongly according to the land cover type, and therefore, changes in cover in the future may have important and currently unknown impacts on the regional CO_2 balance (Marushchak et al. 2013).

Acknowledgments We thank the Department of Earth System Science and Environmental Technologies of the National Council of Research (CNR) for funding the field activities carried out in 2012 and 2013, the research station “Dirigibile Italia” and KingsBay, Vito Vitale and Roberto Sparapani for logistic support, Emiliano Liberatori and Laura Caiazzo for local support. Mauro Guglielmin, Luigi Mazari Villanova, Roberto Gambillara for their help in the field. Luciano

Spaccino for carbon isotope analysis. We thank Prof. Peter Convey for assistance in the English revision of the manuscript.

References

- André M (1993) Les versants du Spitsberg. Presses Universitaires de Nancy, Nancy
- Arndal MF, Illeris L, Michelsen A, Albert K, Tamstorf M, HansenSource BU (2009) Seasonal variation in gross ecosystem production, plant biomass, and carbon and nitrogen pools in five high arctic vegetation types. *Arct Antarct Alp Res* 41:164–173
- Asner JP, Scurlock JMO, Hicke JA (2003) Global synthesis of leaf area index observations: implications for ecological and remote sensing studies. *Glob Ecol Biogeogr* 12:191–205
- Barclay HJ (1998) Conversion of total leaf area to projected leaf area in lodgepole pine and Douglas-fir. *Tree Physiol* 18:185–193
- Bartak M, Vaczi P, Hajek J (2012) Photosynthetic activity in three vascular species of Spitsbergen vegetation during summer season in response to microclimate. *Pol Polar Res* 33:443–462
- Bender MM (1971) Variations in the $^{13}\text{C}/^{12}\text{C}$ ratios of plants in relation to the pathway of photosynthetic carbon dioxide fixation. *Phytochemistry* 10:1239–1244
- Bernacchi CJ, Pimentel C, Long SP (2003) In vivo temperature response functions of parameters required to model RuBP-limited photosynthesis. *Plant, Cell Environ* 26:1419–1430
- Billing WD (1987) Constraints to plant growth, reproduction, and establishment in arctic environments. *Arct Alp Res* 19:357–365
- Björkman MP, Morgner E, Björk RG, Cooper EJ, Elberling B, Klemetsson L (2010) A comparison of annual and seasonal carbon dioxide effluxes between sub-arctic Sweden and high-arctic Svalbard. *Polar Res* 29:75–84
- Bliss LC, Svoboda J (1984) Plant communities and plant production in the western Queen Elizabeth Islands. *Holarct Ecol* 7:325–344
- Boike J, Ippisch O, Overduin PP, Hagedorn B, Roth K (2008) Water, heat and solute dynamics of a mud boil, Spitsbergen. *Geomorphology* 95:61–73
- Brüggemann N, Gessler A, Kayler Z et al (2011) Carbon allocation and carbon isotope fluxes in the plant-soil-atmosphere continuum: a review. *Biogeosciences* 8:3457–3489
- Brugnoli E, Farquhar GD (2000) Photosynthetic Fractionation of Carbon Isotopes. In: Leegood RC, Sharkey TD, von Caemmerer S (eds) *Advances in photosynthesis vol 9: photosynthesis: physiology and metabolism*. Kluwer Academic Publishers, Dordrecht
- Brugnoli E, Scartazza A, Lauteri M, Monteverdi MC, Máguas C (1998) Carbon isotope discrimination in structural and non-structural carbohydrates in relation to productivity and adaptation to unfavourable conditions. *Stable Isotopes*. In: Griffiths H (ed) *Integration of biological, ecological and geochemical processes*. BIOS Scientific Publishers, Oxford, pp 133–144
- Bunce JA (2008) Acclimation of photosynthesis to temperature in *Arabidopsis thaliana* and *Brassica oleracea*. *Photosynth* 46:517–524
- Cannone N, Guglielmin M, Gerdol R (2004) Relationships between vegetation patterns and periglacial landforms in north-western Svalbard. *Polar Biol* 27:562–571
- Cernusak LA, Ubierna N, Winter K, Holtum JAM, Marshall JD, Farquhar GD (2013) Environmental and physiological determinants of carbon isotope discrimination in terrestrial plants. *New Phytol* 200:950–965
- Chapin FS, Woodwell GM, Randerson JT et al (2006) Reconciling carbon—cycle concepts, terminology, and methods. *Ecosystem* 9:1041–1050
- Christiansen CT, Schmidt NM, Michelsen A (2012) High arctic dry heath CO_2 exchange during the early cold season. *Ecosystem* 15:1083–1092
- Elberling B (2007) Annual soil CO_2 effluxes in the high arctic: the role of snow thickness and vegetation type. *Soil Biol Biochem* 39:646–654
- Elvebakk A (1994) A survey of plant associations and alliances from Svalbard. *J Veg Sci* 5:791–802
- Euskirchen ES, Bret-Harte MS, Scott GJ, Edgar C, Shaver GR (2012) Seasonal patterns of carbon dioxide and water fluxes in three representative tundra ecosystems in northern Alaska. *Ecosphere* 3:4. doi:10.1890/ES11-00202.1
- Fan Y, Zhong Z, Zhang X (2011) Determination of photosynthetic parameters $V_{c,max}$ and J_{max} for a C_3 plant (spring hullless barley) at two altitudes on the Tibetan Plateau. *Agric For Meteorol* 151:1481–1487
- Farquhar GD, von Caemmerer S, Berry JA (1980) A biochemical model of photosynthetic CO_2 assimilation in leaves of C_3 species. *Planta* 149:78–90
- Farquhar GD, O’Leary MH, Berry JA (1982) On the relationship between carbon isotope discrimination and the inter-cellular carbon-dioxide concentration in leaves. *Aust J Plant Physiol* 9:121–137
- Farquhar GD, Ehleringer JR, Hubic KT (1989) Carbon isotope discrimination and photosynthesis. *Annu Rev Plant Physiol Plant Mol Biol* 40:503–537
- Groendahl L, Friborg T, Soegaard H (2007) Temperature and snow-melt controls on interannual variability in carbon exchange in the high arctic. *Theor Appl Clim* 88:111–125
- Heimann M, Reichstein M (2008) Terrestrial ecosystem carbon dynamics and climate feedbacks. *Nature* 451:289–292
- IPCC (2013) Summary for policymakers. In: Stocker TF et al (eds) *Climate change 2013: the physical science basis. Contribution of working group I to the fifth assessment report of the intergovernmental panel on climate change*. Cambridge University Press, Cambridge, United Kingdom and New York, NY, USA
- Kirschbaum MUF (2004) Soil respiration under prolonged soil warming: are rate reductions caused by acclimation or substrate loss? *Glob Chang Biol* 10:1870–1877
- Körner C (2006) Plant CO_2 responses: an issue of definition, time and resource supply. *New Phytol* 172:393–411
- Kositsup B, Montpied P, Kasemsap P, Thaler P, Amélio T, Dreyer E (2009) Photosynthetic capacity and temperature responses of photosynthesis of rubber trees (*Hevea brasiliensis* Müll. Arg.) acclimate to changes in ambient temperatures. *Trees Struct Funct* 23:357–365
- Koven CD, Ringeval B, Friedlingstein P et al (2011) Permafrost carbon-climate feedbacks accelerate global warming. *PNAS* 108:14769–14774
- Lafleur PM, Humphreys ER (2008) Spring warming and carbon dioxide exchange over low Arctic tundra. *Glob Chang Biol* 14:740–756
- Lafleur PM, Humphreys ER, St. Louis VL et al (2012) Variation in peak growing season net ecosystem production across the Canadian arctic. *Environ Sci Technol* 46:7971–7977
- Lloyd CR (2001) The measurement and modeling of the carbon dioxide exchange at a high arctic site in Svalbard. *Glob Chang Biol* 7:405–426
- Long SP, Bernacchi CJ (2003) Gas exchange measurements, what can they tell us about the underlying limitations to photosynthesis? Procedures and sources of error. *J Exp Bot* 54(392):2393–2401
- Lüers J, Westermann S, Piel K, Boike J (2014) Annual CO_2 budget and seasonal CO_2 exchange signals at a high arctic permafrost site on Spitsbergen, Svalbard archipelago. *Biogeosciences* 11:6307–6322

- Lund M et al (2010) Variability in exchange of CO₂ across 12 northern peatland and tundra sites. *Glob Chang Biol* 16:2436–2448
- Marushchak ME, Kiepe I, Biasi C et al (2013) Carbon dioxide balance of subarctic tundra from plot to regional scales. *Biogeosciences* 10:437–452
- McFadden JP, Eugster W, Chapin FS (2003) A regional study of the controls on water vapor and CO₂ exchange in Arctic tundra. *Ecology* 84:2762–2776
- McGuire AD, Anderson LG, Christensen TR et al (2009) Sensitivity of the carbon cycle in the Arctic to climate change. *Ecol Monogr* 79:523–555
- McGuire AD, Christensen TR, Hayes D et al (2012) An assessment of the carbon balance of Arctic tundra: comparisons among observations, process models, and atmospheric inversions. *Biogeosciences* 9:3185–3204
- Molau U, Molgaard P (eds) (1996) ITEX manual. Danish Polar Center, Denmark. ISBN 87-90369-04-1
- Morgner E, Elberling B, Strebel D, Cooper EJ (2010) The importance of winter in annual ecosystem respiration in the high arctic: effects of snow depth in two vegetation types. *Polar Res* 29:58–74
- Muraoka H, Noda H, Uchida M, Ohtsuka T, Koizumi H, Nakatsubo T (2008) Photosynthetic characteristics and biomass distribution of the dominant vascular plant species in a high arctic tundra ecosystem, Ny-Ålesund, Svalbard: implications for their role in ecosystem carbon gain. *J Plant Res* 121:137–145
- Nakatsubo T, Fujiyoshi M, Yoshitake S, Koizumi H, Uchida M (2010) Colonization of the polar willow *Salix polaris* on the early stage of succession after glacier retreat in the high arctic, Ny-Alesund, Svalbard. *Polar Res* 29:385–390. doi:10.1111/j.1751-8369.2010.00170.x
- Nelson DW, Sommers LE (1996) Total carbon, organic carbon, and organic matter. In: Bigham JM et al (eds) Soil Science Society of America and American Society of Agronomy. Methods of soil analysis. Part 3: chemical methods-SSSA. Book series no. 5. Madison, WI, Chapter 34, pp 1001–1006
- Norby RJ, Luo Y (2004) Evaluating ecosystem responses to rising atmospheric CO₂ and global warming in a multi-factor world. *New Phytol* 162:281–293
- Nowak RS, Ellsworth DS, Smith SD (2004) Functional responses of plants to elevated atmospheric CO₂—do photosynthetic and productivity data from FACE experiments support early predictions? *New Phytol* 162:253–280
- O’Leary MH (1981) Carbon isotope fractionation in plants. *Phytochemistry* 27:553–567
- Oberbauer SF, Tweedie CE, Welker JM et al (2007) Tundra CO₂ fluxes in response to experimental warming across latitudinal and moisture gradients. *Ecol Monogr* 77:221–238
- Possell M, Hewitt CN (2009) Gas exchange and photosynthetic performance of the tropical tree *Acacia nigrescens* when grown in different CO₂ concentrations. *Planta* 229:837–846
- Rønning OI (1986) The flora of Svalbard. Norsk Polar Institutt, Oslo
- Schmidt H-L, Robins RJ, Werner RA (2015) Multi factorial in vivo stable isotope fractionation: causes, correlations, consequences and applications. *Isotopes Environ Health Stud* 51:155–199
- Shaver GR, Rastetter EB, Salmon V et al (2013) Pan-Arctic modelling of net ecosystem exchange of CO₂. *Philos Trans R Soc B* 368:20120485
- Sjögerstern S, van der Wal R, Woodin SJ (2006) Small-scale hydrological variation determines landscape CO₂ fluxes in the high arctic. *Biogeochem* 80:205–216
- Tarnocai C, Canadell JG, Schuur EAG, Kuhry P, Mazhitova G, Zimov SA (2009) Soil organic carbon pools in the northern circumpolar permafrost region. *Global Biogeochem Cycles*. doi:10.1029/2008GB003327
- Uchida M, Kishimoto A, Muraoka H (2010) Seasonal shift in factors controlling net ecosystem production in a high arctic terrestrial ecosystems. *J Plant Res* 123:79–85
- Welker JM, Fahnestock JT, Henry GHR et al (2004) CO₂ exchange in three Canadian high arctic ecosystems: response to long-term experimental warming. *Glob Chang Biol* 10:1981–1995
- Yoshitake S, Uchida M, Koizumi H, Kanda H, Nakatsubo T (2010) Production of biological soil crusts in the early stage of primary succession on a high arctic glacier foreland. *New Phytol* 186:451–460